

Porphyrinoids

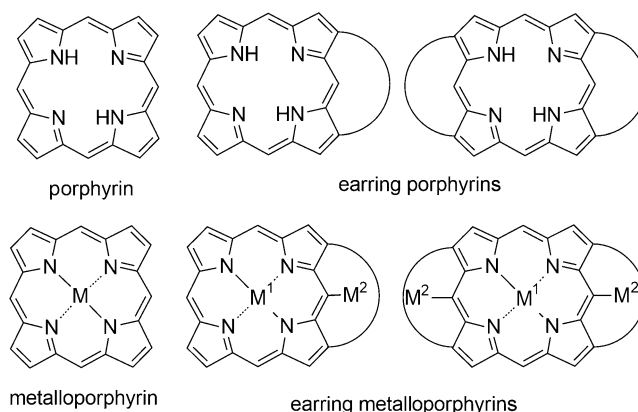
International Edition: DOI: 10.1002/anie.201600955
German Edition: DOI: 10.1002/ange.201600955

π -Extended “Earring” Porphyrins with Multiple Cavities and Near-Infrared Absorption

Yutao Rao, Taeyeon Kim, Kyu Hyung Park, Fulei Peng, Lei Liu, Yunmei Liu, Bin Wen, Shubin Liu, Steven Robert Kirk, Licheng Wu, Bo Chen, Ming Ma, Mingbo Zhou, Bangshao Yin, Yuexing Zhang, Dongho Kim,* and Jianxin Song*

Abstract: β,β -tripyrin-bridged earring porphyrins were synthesized through Suzuki–Miyaura cross coupling reactions. These porphyrinoids have multiple cavities and can accommodate two or three metal ions per molecule. The structures of the porphyrins have been elucidated by x-ray diffraction analysis, and feature curved π planes. The electronic spectra of the porphyrins exhibit near-infrared (NIR) absorptions and metal insertion leads to red-shifted and intensified absorption features. Electrochemical analysis and transient absorption measurements indicated that the porphyrins exhibit effective electronic communication between their central and peripheral moieties.

Porphyrins, with their fascinating π -conjugated systems, are favorable candidates for use in optoelectronic devices, sensors, photovoltaic devices, pigments for phototherapy, and nonlinear optical materials.^[1] Modification of porphyrin structures and manipulation of electronic interactions have attracted much attention in recent years.^[2] Porphyrins have a central cavity that can accommodate one metal ion, while expanded porphyrins have a much more flexible and larger cavity that can accommodate one or more metal ions or phosphorous atoms.^[3] Herein we report the synthesis of β,β -tripyrin-bridged “earring” porphyrins (Scheme 1) which possess multiple cavities and can complex up to three metal



Scheme 1. Structures of porphyrins, earring porphyrins, and their metal complexes.

ions. The side “ear” cavity of the earring porphyrin also acts as a carbaporphyrinoid system, so we postulate that the “ear” could exhibit some similar properties to carbaporphyrins.^[4] The earring metalloporphyrins are also similar to porphyrin pincer molecules that may have potential catalytic activity.^[2]

To the best of our knowledge, a porphyrinoid monomer with two or even three cavities has not been reported to date. The short distance between the “ear” and the “face” means that the metal insertion can effectively extend the electronic conjugated systems and trigger activation of the electronic interaction between the porphyrin (“face”) and the connected tripyrrin (“ear”). Diboryltripyrane **1** was synthesized through Ir-catalyzed borylation of a tripyrrane precursor.^[5] β,β' -dibromo Ni^{II} porphyrin **2a** was synthesized as previously reported.^[6] With **1** and **2a** in hand, **4a** was prepared smoothly through the Suzuki–Miyaura reaction (Scheme 2). After oxidation and purification, **4a** was obtained in 30 % yield. Although β,β' -diboryl Ni^{II} porphyrin and dibromotripyrrin precursors are more easily synthesized than **1** and **2a**,^[2a] neither of the target molecules was obtained. Earring porphyrin **4a** has a newly formed second cavity which could accommodate a metal ion. In fact, treatment of **4a** with $\text{Pd}(\text{OAc})_2$ in dichloromethane/methanol at room temperature resulted in facile metalation to provide metal complex **4a-Pd** in 95 % yield. The structures of **4a** and **4a-Pd** have been assigned by their high-resolution ESI-TOF mass and ^1H NMR spectra.^[8] The final structural confirmation of **4a** and **4a-Pd** were obtained from single-crystal X-ray diffraction analysis (Figure 1 b,d).^[7] Compound **4a** has a smoothly curved plane and the maximum displacement of the porphyrin plane is

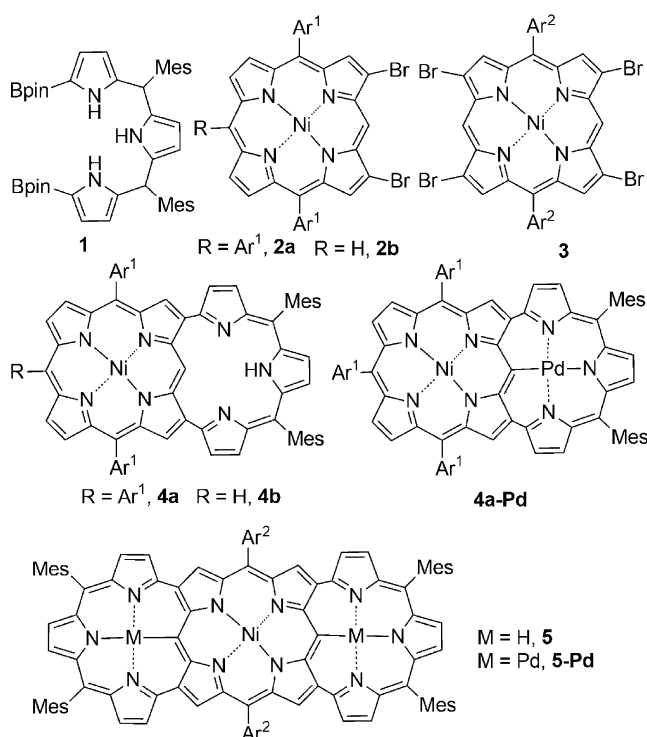
[*] Y. Rao, F. Peng, L. Liu, Y. Liu, B. Wen, Prof. Dr. S. Liu, Prof. Dr. S. R. Kirk, L. Wu, Prof. Dr. B. Chen, Prof. Dr. M. Ma, Dr. M. Zhou, Dr. B. Yin, Prof. Dr. J. Song
Key Laboratory of Chemical Biology and Traditional Chinese Medicine Research (Ministry of Education of China), Key Laboratory of Application and Assemble of Organic Functional Molecules Hunan Normal University, Changsha 410081 (China)
E-mail: jxsong@hunnu.edu.cn

T. Kim, K. H. Park, Prof. Dr. D. Kim
Spectroscopy Laboratory for Functional π -Electronic Systems and Department of Chemistry, Yonsei University
Seoul 03722 (Korea)
E-mail: dongho@yonsei.ac.kr

Dr. Y. Zhang
Department of Chemistry and Pharmaceutical Sciences, Guangxi Normal University, Key Laboratory for the Chemistry and Molecular Engineering of Medicinal Resources (Ministry of Education)
15 Yucai Road, Guilin 541004 (China)

Prof. Dr. S. Liu
Division of Research Computing, Information Technology Services
University of North Carolina
Chapel Hill, NC 27599 (USA)

Supporting information for this article can be found under:
<http://dx.doi.org/10.1002/anie.201600955>.



Scheme 2. Reported compounds. Ar¹ = 3,5-di-*tert*-butylphenyl, Ar² = 3,5-di-dodecyloxyphenyl, Bpin = pinacolboronate, M = metal, Mes = 2,4,6-trimethylphenyl.

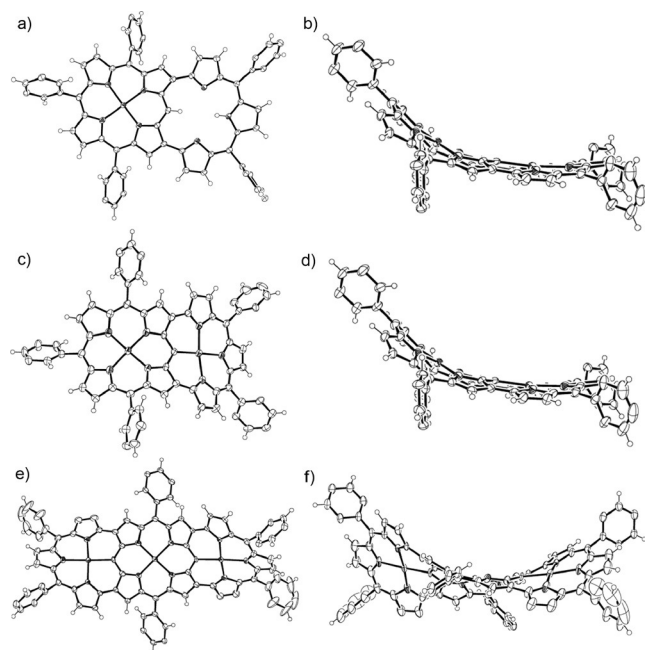


Figure 1. X-ray crystal structures of earring porphyrins. a) Top view of **4a**, b) side view of **4a**, c) top view of **4a-Pd**, d) side view of **4a-Pd**, e) top view of **5-Pd**, and f) side view of **5-Pd**. Thermal ellipsoids are at the 50% probability level. Alkyl and alkoxy groups and solvent molecules are omitted for clarity. Disorder was found for aryl and alkoxy groups in **5-Pd**.

0.659(3) Å from the meso carbon atom. Both the C–N distance 4.505(3) Å and the N–N distance 4.064(4) Å of the newly formed cavity are longer than the N–N distance (ca. 3.84 Å) of porphyrin, so the new cavity is bigger than the porphyrin central cavity. The dihedral angle between the “face” and the “ear” is 162.12(4)°, and the N–C–Ni angle is 175.33(9)°. The C–C distance between “face” and the “ear” is 1.450(3) Å for **4a**, 1.409(7) Å for **4a-Pd**.^[8]

In **4a-Pd**, Pd^{II} insertion resulted in an increase of the maximum displacement of the porphyrin plane to 0.759(4) Å, a decrease in the dihedral angle between the “face” and the “ear” to 150.5677(4)°, and a decrease in the N–C–Ni angle to 166.5687(4)°, thus inducing further curvature of the earring porphyrin. The C–N and N–N distances of the second cavity are also shortened to 4.14724(9) and 4.05732(4) Å, respectively. In order to expand this synthetic strategy, we attempted to synthesize double earring porphyrin from **1** and β-tetrabromoporphyrin. Firstly, synthesis of β-tetrabromoporphyrin from β-tetraboryl-5,10 bis(3,5-di-*tert*-butyl) Ni^{II} porphyrin failed and resulted in mixtures with poor solubility. Then we tried to synthesize the target molecule in a stepwise reaction from **4b**, which was prepared from **1** and **2b**. After borylation and bromination of **4b**, β,β′-dibrominated **4b** was obtained in poor yield. Finally, we sought to synthesize β-tetrabromoporphyrin again. After changing the *tert*-butyl group on phenyl the phenyl substituent to an alkoxy group,^[9] β-tetrabromoporphyrin **3** was successfully obtained in 85% yield. The double earring porphyrin **5** was then prepared in 15% yield from the cross-coupling reaction of **3** and **1**. The parent ion peak of **5** was observed at *m/z* 2163.2833 (calculated for [C₁₄₄H₁₇₀N₁₀NiO₄]⁺ 2163.2816 ([M]⁺)) in the high resolution MALDI-TOF mass spectrum. The ¹H NMR spectrum of **5** in CDCl₃ at 25°C shows singlet peaks at δ = 17.18 and 15.9 ppm that arise from the meso-H and N–H protons, respectively. Compound **5** could coordinate with a Ni^{II} ion in the central cavity, and the two carbaporphyrinoid cavities remained empty. Treatment of **5** with Pd(OAc)₂ in dichloromethane/methanol at room temperature provided the metal complex **5-Pd** in 90% yield. The structure of **5-Pd** was assigned from its high-resolution ESI-TOF mass and ¹H NMR spectra.^[8] Fortunately, a crystal of **5-Pd** suitable for single-crystal X-ray diffraction analysis was obtained by slow solvent diffusion of heptane to its solution in dichloroethane (Figure 1 e, f). The earring porphyrin **5-Pd** has a curvature that is much bigger than that of **4a** and **4a-Pd**, with a “face”–“ear” dihedral angle of 142.29(8)°, while the two “ears” are almost perpendicular to each other, with a 75.26(4)° dihedral angle. The structure of **5-Pd** is very interesting as the molecule exhibits a helical “s” conformation, the maximum displacement of the mean plane of the “ear” is 0.625(7) Å while that of the mean plane of the “face” is 1.071(5) Å, the Ni–Pd distance is 5.4966(4) Å and the Pd–Pd distance is 10.9254(8) Å. The C–C distance between “face” and “ears” is 1.420(8) Å.^[8]

The ¹H NMR spectra and nucleus-independent chemical shift (NICS) calculations indicated that the aromatic pathways of these earring porphyrins do not extend over the entire molecule; two regions are separated in terms of aromaticity/antiaromaticity. The porphyrin core is aromatic but the side

moiety is antiaromatic, as supported by the significant deshielding of the N–H unit ($\delta \approx 17.5$ ppm) and NICS calculations.^[8] Further investigation of the aromaticity/antiaromaticity of earring porphyrins will be reported elsewhere.

The UV/Vis/NIR absorption spectra of earring porphyrins measured in CH_2Cl_2 are shown in Figure 2. The absorption spectra of **4a** and **5** are similar, showing broader Soret bands and red-shifted Q-like bands as compared with porphyrin monomers. Both **4a** and **5** exhibit absorption features with a weak Q-band tail which extends into the near infrared spectral region (up to 900 nm). In sharp contrast, that of **4a-Pd** and **5-Pd** show remarkably near-infrared absorptions from 700 to 1500 nm (Figure 2, inset), arising from effective π -conjugation upon Pd^{II} insertion. Density functional theory (DFT) calculations also revealed distinct differences between the molecular orbitals of **4a** (**5**) and **4a-Pd** (**5-Pd**).^[8] Also more ruffled structures of Ni^{II} porphyrin moieties upon Pd^{II} insertion have directly affected their electronic structures, as evidenced by further red-shifted absorption spectral features.^[10]

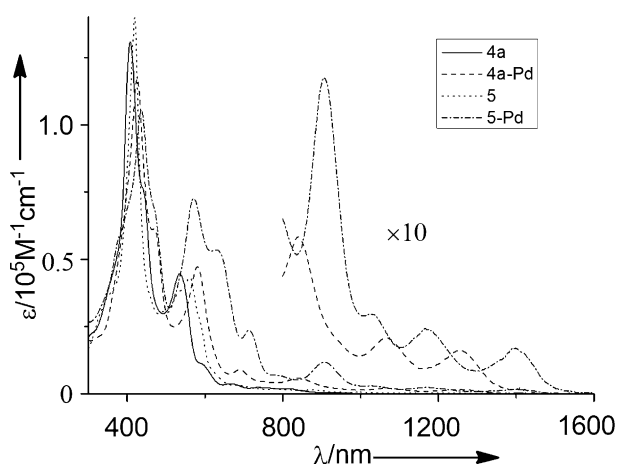


Figure 2. UV/Vis/NIR absorption spectra of earring porphyrins **4a**, **5**, **4a-Pd**, and **5-Pd** in CH_2Cl_2 . The inset shows the enlarged Q-like bands in the absorption spectra of earring porphyrins.

In order to gain further insight into their electronic properties, electrochemical analysis was performed.^[8] The results of cyclic voltammetry measurements for **4a**, **4a-Pd**, **5**, **5-Pd** are summarized in Table 1. The reference Ni^{II} porphyrin monomer exhibits an oxidation potential at 0.48 V and a reduction potential at -1.83 V, and the electrochemical HOMO–LUMO gap can be estimated to be 2.31 eV. The electrochemical HOMO–LUMO gaps of these earring porphyrins are significantly lower than 2.31 eV. Both oxidation and reduction potentials of these earring porphyrins were split, thus indicating the presence of effective electronic communication between the “face” and “ear” moieties. The first oxidation potential (vs. Fc/Fc^+) is decreased from 0.38 V for **4a** to 0.21 V for **4a-Pd**, and the first reduction potential is increased from -1.23 V for **4a** to -0.99 V for **4a-Pd**. For **5a** and **5a-Pd**, we also observed the same trend, which results in a substantial decrease of the HOMO–LUMO gap by metalation of the side cavities. The optical HOMO–LUMO gaps

Table 1: Summary of electrochemical potentials.

Compound	$E_{\text{ox},1}$	$E_{\text{red},1}$	$\Delta E_{\text{HL}}^{[a]}$	$\Delta E_{\text{op}}^{[b]}$
Reference ^[c]	0.48	-1.83	2.31	2.36
4a	0.38	-1.23	1.61	1.32
5	0.38	-1.13	1.51	1.24
4a-Pd	0.21	-0.99	1.20	0.99
5-Pd	0.16	-0.90	1.06	0.88

[a] Electrochemical HOMO–LUMO gap, $\Delta E_{\text{HL}} = E_{\text{ox},1} - E_{\text{red},1}$ (vs. Fc/Fc^+);

[b] ΔE_{op} was calculated from the absorption spectra; [c] 5,10,15-tri(3,5-di-*tert*-butylphenyl)porphyrinato nickel(II) monomer.

estimated from the absorption maxima are in full agreement with the electrochemistry results. Density functional theory (DFT) calculations also revealed distinct differences between the molecular orbitals of Ni^{II} porphyrin, earring porphyrins (**4a**, **5**), and earring Pd^{II} porphyrins (**4a-Pd**, **5-Pd**).^[8] These results reveal effective delocalization of the π -electronic system after modifying the molecular structure through 1) connection of porphyrin with tripyrrin to form the earring porphyrin and 2) Pd^{II} insertion into the side cavity. Figure S22 in the Supporting Information shows that the order of the gaps obtained from the simulation agrees well with that from our experimental findings.

To investigate the excited-state dynamics of a series of earring porphyrins, we carried out femtosecond transient absorption (fs-TA) measurements. Firstly, we measured the fs-TA spectra of the reference monomer. The TA spectra of the reference monomer exhibit typical characteristic features of Ni^{II} porphyrinoids, namely overall blue-shifted excited-state absorption (ESA) with a sharpened shape, which is a characteristic feature when the (d,d) state is rapidly populated upon photoexcitation. This spectral signature is indicative of fast deactivation from the $S_1(\pi,\pi^*)$ state to the vibrationally hot (d,d) states followed by a cooling process to the lowest (d,d) state and subsequently a relatively slow relaxation from the lowest (d,d) state to the ground state (Figure S28).^[11] As shown in the TA spectra and their decay profiles of **4a** and **5** (Figure S26), we also could partly observe similar spectral features of Ni^{II} porphyrinoids except for very fast deactivation of $S_1(\pi,\pi^*)$ state to the (d,d) state. This feature presumably originates from strongly perturbed electronic structures of earring porphyrins by a direct connection between Ni^{II} porphyrin and earring moieties. Nevertheless, the TA spectra of **4a** and **5** exhibit small spectral shifts arising from the vibrational cooling processes (3.8 and 5.4 ps) in the (d,d) state followed by relaxation from the lowest (d,d) states to the ground state. The TA spectra and their decay profiles of **4a-Pd** and **5-Pd** are shown in Figure S27. They are too complicated for the assignment of excited-state dynamics as Pd^{II} insertion results in heterometallic species that allow more electronic interactions between the (d,d) and (π,π^*) states than those that contain only Ni^{II} metal (**4a** and **5**). However, the TA spectra do show several distinct features compared with compounds **4a** and **5**. In particular, unlike the spectral shifts shown in the ESA region for monomer, **4a**, and **5**, the TA spectra of Pd^{II} -inserted earring porphyrins (**4a-Pd** and **5-Pd**) were shifted into the blue region and then back again into the red to the ESA signals at around 525 and 650 nm.

Furthermore, the fastest decay components of 0.9 ps^{-1} and 0.4 ps^{-1} are assumed to be rate constants for the newly formed intersystem crossing (ISC) pathways which arise from a heavy-atom effect induced by Pd^{II} and were therefore not observed in **4a** and **5**. Thus, upon photoexcitation, a competition between deactivation pathways occurs; one for the $S_1(\pi, \pi^*)$ decay to the vibrationally hot (d,d) states in Ni^{II} and the other for the $S_1(\pi, \pi^*)$ deactivation by ISC, and then followed by cooling processes (7.7 and 2.5 ps) and subsequently relaxation to the ground state (345 and 435 ps). Although, the excited-state dynamics of a series of metalated earring porphyrins have been explored by TA measurements, the exact determination of the interplay between the excited states still remains to be clearly determined. Correspondingly, further investigations on other types of earring porphyrins are currently underway.

In summary, β, β -tripyrin-bridged earring porphyrins have been synthesized through Suzuki–Miyaura coupling reactions. These earring porphyrins have two or three cavities that can each accommodate a metal ion. The structures of these earring porphyrins have been elucidated by X-ray diffraction analysis. These earring porphyrins exhibit near-infrared (NIR) absorptions and curved π planes. Metalation causes a further red-shift in and increases the intensity of the NIR absorption, and results in an increase in the curvature of the molecule. Electrochemical analysis and TA measurements indicated that the porphyrins exhibit effective electronic communication between the “face” and “ear” moieties. The present work is an important advance towards developing new porphyrinoids with NIR absorption and multimetal coordinative properties. Exploration of their metal coordinative, magnetic, photophysical, aromaticity/antiaromaticity, and catalytic properties and development of new earring porphyrins are ongoing.

Acknowledgements

We thank Dr. Zier Yan (Rigaku Beijing Corporation, China) for help in crystallographic analysis. The work at Hunan Normal University was supported by the National Natural Science Foundation of China. (Grant No. 21272065), the Scientific Research Foundation for the Returned Overseas Chinese Scholars, State Education Ministry, and Scientific Research Fund of Hunan Provincial Education Department (Grant No.13k027). The research at Yonsei University was supported by the Global Research Laboratory (GRL) Program (2013K1A1A2A02050183) of the Ministry of Education, Science and Technology (MEST) of Korea.

Keywords: conjugation · near-infrared absorption · nickel · palladium · porphyrinoids

How to cite: *Angew. Chem. Int. Ed.* **2016**, *55*, 6438–6442
Angew. Chem. **2016**, *128*, 6548–6552

- [1] a) T. Tanaka, A. Osuka, *Chem. Soc. Rev.* **2015**, *44*, 943; b) M. Pawlicki, H. A. Collins, R. G. Denning, H. L. Anderson, *Angew. Chem. Int. Ed.* **2009**, *48*, 3244; *Angew. Chem.* **2009**, *121*, 3292;

- c) N. Aratani, D. Kim, A. Osuka, *Chem. Asian J.* **2009**, *4*, 1172; d) D. Holten, D. F. Bocian, J. S. Lindsey, *Acc. Chem. Res.* **2002**, *35*, 57; e) A. Tsuda, A. Osuka, *Science* **2001**, *293*, 79; f) D. Gust, T. A. Moore, A. L. Moore, *Acc. Chem. Res.* **2001**, *34*, 40; g) D. Gust, T. A. Moore, A. L. Moore, *Acc. Chem. Res.* **1993**, *26*, 198; h) M. R. Wasielewski, *Chem. Rev.* **1992**, *92*, 435; i) M. Urbani, M. Grätzel, K. M. Nazeeruddin, T. Torres, *Chem. Rev.* **2014**, *114*, 12330.
- [2] a) K. Oda, M. Akita, S. Hiroto, H. Shinokubo, *Org. Lett.* **2014**, *16*, 1818; b) Q. Chen, Y. Zhu, Q. Fan, S. Zhang, J. Zheng, *Org. Lett.* **2014**, *16*, 1590; c) H. Mori, J. M. Lim, D. Kim, A. Osuka, *Angew. Chem. Int. Ed.* **2013**, *52*, 12997; *Angew. Chem.* **2013**, *125*, 13235; d) H. Yorimitsu, A. Osuka, *Asian J. Org. Chem.* **2013**, *2*, 356; e) K. Fujimoto, H. Yorimitsu, A. Osuka, *Org. Lett.* **2014**, *16*, 972; f) S. Anabuki, H. Shinokubo, N. Aratani, A. Osuka, *Angew. Chem. Int. Ed.* **2012**, *51*, 3174; *Angew. Chem.* **2012**, *124*, 3228; g) M. O. Senge, *Chem. Commun.* **2011**, *47*, 1943; h) Y. Matano, K. Matsumoto, H. Hayashi, Y. Nakao, T. Kumpulainen, V. Chukharev, N. V. Tkachenko, H. Lemmetyinen, S. Shimizu, N. Kobayashi, D. Sakamaki, A. Ito, K. Tanaka, H. Imahori, *J. Am. Chem. Soc.* **2012**, *134*, 1825; i) H. Shinokubo, A. Osuka, *Chem. Commun.* **2009**, 1011; j) S. Yamaguchi, T. Katoh, H. Shinokubo, A. Osuka, *J. Am. Chem. Soc.* **2007**, *129*, 6392; k) H. Hata, H. Shinokubo, A. Osuka, *J. Am. Chem. Soc.* **2005**, *127*, 8264; l) N. K. S. Davis, A. L. Thompson, H. L. Anderson, *J. Am. Chem. Soc.* **2011**, *133*, 30.
- [3] a) S. Shimizu, V. J. Anand, R. Taniguchi, K. Furukawa, T. Kato, T. Yokoyama, A. Osuka, *J. Am. Chem. Soc.* **2004**, *126*, 12280; b) H. Rath, S. Tokui, N. Aratani, K. Furukawa, J. M. Lim, D. Kim, H. Shinokubo, A. Osuka, *Angew. Chem. Int. Ed.* **2010**, *49*, 1489; *Angew. Chem.* **2010**, *122*, 1531; c) S. Mori, A. Osuka, *J. Am. Chem. Soc.* **2005**, *127*, 8030; d) S. Mori, A. Osuka, *Inorg. Chem.* **2008**, *47*, 3937; e) T. Higashino, J. M. Lin, T. Miura, S. Saito, J.-Y. Shin, D. Kim, A. Osuka, *Angew. Chem. Int. Ed.* **2012**, *51*, 13105; *Angew. Chem.* **2012**, *124*, 13282; f) S. Hannah, D. Seidel, J. S. Sessler, V. Lynch, *Inorg. Chim. Acta* **2001**, *317*, 211.
- [4] a) D. I. AbuSalim, G. M. Ferrence, T. D. Lash, *J. Am. Chem. Soc.* **2014**, *136*, 6763; b) R. Li, A. D. Lammer, G. M. Ferrence, T. D. Lash, *J. Org. Chem.* **2014**, *79*, 4078; c) D. Li, T. D. Lash, *J. Org. Chem.* **2014**, *79*, 7112; d) D. I. Abusalim, T. D. Lash, *J. Org. Chem.* **2013**, *78*, 11535; e) T. D. Lash, A. D. Lammer, G. M. Ferrence, *Angew. Chem. Int. Ed.* **2012**, *51*, 10871; *Angew. Chem.* **2012**, *124*, 11029.
- [5] a) J. Setsune, M. Toda, M. K. Watan, P. K. Pandab, T. Yoshidab, *Tetrahedron Lett.* **2006**, *47*, 7541; b) K. Mertins, A. Zapf, M. Beller, *J. Mol. Catal. A* **2004**, *207*, 21; c) T. Ishiyama, J. Takagi, Y. Yonekawa, J. F. Hartwig, N. Miyaura, *Adv. Synth. Catal.* **2003**, *345*, 1103.
- [6] H. Cai, K. Fujimoto, J. M. Lim, C. Wang, W. Huang, Y. Tao, S. Zhang, H. Shi, B. Yin, B. Chen, M. Ma, J. Song, D. Kim, A. Osuka, *Angew. Chem. Int. Ed.* **2014**, *53*, 11088; *Angew. Chem.* **2014**, *126*, 11268.
- [7] Crystal data for **4a**: $\text{C}_{103}\text{H}_{105}\text{Cl}_{1.5}\text{N}_7\text{Ni}$, $M_w = 1552.82$, triclinic, space group $P\bar{1}$, $a = 12.9479(3)$, $b = 17.4776(4)$ Å, $c = 20.9002(4)$, $\alpha = 106.0910(19)$, $\beta = 99.3043(17)$, $\gamma = 103.119(2)^\circ$, $V = 4296.38(18)$ Å³, $Z = 2$, $D_{\text{calc}} = 1.200\text{ g cm}^{-3}$, $T = 100(2)$ K, 47178 measured reflections, 16711 unique reflections, $R = 0.0640$, $R_w = 0.1805$ (all data), $\text{GOF} = 1.028$ ($I > 2.0\sigma(I)$). Crystal data for **4a-Pd**: $\text{C}_{94}\text{H}_{97}\text{N}_7\text{NiPd}$, $M_w = 1489.90$, monoclinic, space group $P1\ 21/c1$, $a = 23.0793(8)$, $b = 15.2187(4)$, $c = 27.0655(6)$ Å, $\alpha = 90$, $\beta = 95.459(3)$, $\gamma = 90^\circ$, $V = 9463.3(5)$ Å³, $Z = 4$, $D_{\text{calc}} = 1.046\text{ g cm}^{-3}$, $T = 173(2)$ K, 32689 measured reflections, 14764 unique reflections, $R = 0.0634$, $R_w = 0.1748$ (all data), $\text{GOF} = 1.039$ ($I > 2.0\sigma(I)$). Crystal data for **5-Pd**: $\text{C}_{144}\text{H}_{128}\text{N}_{10}\text{NiO}_4\text{Pd}_2$, $M_w = 2334.07$, monoclinic, space group $C1\ 2/c1$, $a = 27.6852(4)$, $b = 24.0258(6)$, $c = 22.5943(3)$ Å, $\alpha = 90$, $\beta = 111.6319(16)$, $\gamma = 90^\circ$, $V = 13970.4(5)$ Å³, $Z = 4$, $D_{\text{calc}} = 1.112\text{ g cm}^{-3}$, $T = 100.01(10)$ K, 37658 mea-

sured reflections, 12452 unique reflections, $R=0.0647$, $R_w=0.1840$ (all data), $GOF=1.015$ ($I>2.0\sigma(I)$). CCDC1446008 (**4a**), 1446007 (**4a-Pd**) and 1446009 (**5-Pd**) contain the supplementary crystallographic data for this paper. These data can be obtained free of charge from The Cambridge Crystallographic Data Centre.

[8] For details, see the Supporting Information.

[9] N. Aratani, A. Takagi, Y. Yanagawa, T. Matsumoto, T. Kawai, Z. S. Yoon, D. Kim, A. Osuka, *Chem. Eur. J.* **2005**, *11*, 3389.

[10] R. E. Haddad, S. Gazeau, J. Pecaut, J.-C. Marchon, C. J. Medforth, J. A. Shelnutt, *J. Am. Chem. Soc.* **2003**, *125*, 1253.

[11] C. M. Drain, C. Kirmaier, C. J. Medforth, D. J. Nurco, K. M. Smith, D. Holtz, *J. Phys. Chem.* **1996**, *100*, 11984.

Received: January 27, 2016

Revised: March 8, 2016

Published online: April 1, 2016